OPTICAL PRODUCTION OF NEGATIVE IONS

Report for period
15 Jul 87-
14 Dec 88

Contract No. F49620-87-C-0080

prepared for

AIR FORCE OFFICE OF SCIENTIFIC RESEARCH
Bolling Air Force Base
Washington, DC 20332-6448

by

AVCO RESEARCH LABORATORY, INC.
a subsidiary of Textron, Inc.
2385 Revere Beach Parkway
Everett, Massachusetts 02149

UNCLASSIFIED

SECURITY CLASSIFICATION OF THIS PAGE (When Data Entered)

REPORT DOCUMENTATION PAGE		READ INSTRUCTIONS BEFORE COMPLETING FORM
1. REPORT NUMBER AFOSR-TR- 89-0812	2. GOVT ACCESSION NO.	3. RECIPIENT'S CATALOG NUMBER
4. TITLE (and Subtitle) OPTICAL PRODUCTION OF NEGATIVE IONS		5. TYPE OF REPORT & PERIOD COVERED FINAL 15 Jul 87 - 14 Dec 88
		6. PERFORMING ORG. REPORT NUMBER
7. AUTHOR(s) M.W. McGeoch		8. CONTRACT OR GRANT NUMBER(s) F49620-87-C-0080
9. PERFORMING ORGANIZATION NAME AND ADDRESS Avco Research Laboratory/Textron 2385 Revere Beach Parkway Everett, MA 02149		10. PROGRAM ELEMENT, PROJECT, TASK AREA & WORK UNIT NUMBERS 61102F, 2301/A7
11. CONTROLLING OFFICE NAME AND ADDRESS Same as 14		12. REPORT DATE Feb '89
		13. NUMBER OF PAGES 29
14. MONITORING AGENCY NAME & ADDRESS (if different from Controlling Office) Air Force Office of Scientific Research Bolling Air Force Base Washington, DC 20332-6448 NP		15. SECURITY CLASS. (of this report) UNCLASSIFIED
		15a. DECLASSIFICATION/DOWNGRADING SCHEDULE

16. DISTRIBUTION STATEMENT (of this Report)

Approved for public release; distribution unlimited.

17. DISTRIBUTION STATEMENT (of the abstract entered in Block 20, if different from Report)

18. SUPPLEMENTARY NOTES

19. KEY WORDS (Continue on reverse side if necessary and identify by block number)

Negative Ions, Lithium, Optical Plasma

20. ABSTRACT (Continue on reverse side if necessary and identify by block number)

A kinetic model of an optically pumped lithium plasma is discussed. Observations of ionization processes at high Rydberg atom density are analyzed, and the role of an electron avalanche process is identified. The optical pump intensity requirements for continuous plasma formation are derived, and Li^- production is modeled.

DD FORM 1 JAN 73 1473 EDITION OF 1 NOV 65 IS OBSOLETE

UNCLASSIFIED

SECURITY CLASSIFICATION OF THIS PAGE (When Data Entered)

TABLE OF CONTENTS

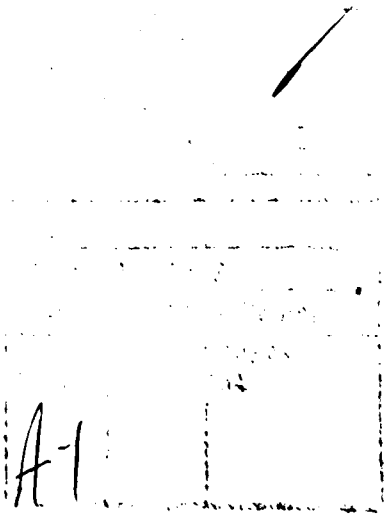

LIST OF ILLUSTRATIONS

1.0 INTRODUCTION

The present work is the continuation of a study of processes leading to the production of negative ions in an optically-pumped plasma. In the prior reporting period a search had been made for the ion pair production process:

$$Li^{**} + Li^{**} \rightarrow Li^{+} + Li^{-} \qquad (1)$$

which involves the collision of two Rydberg atoms prepared by optical pumping. In spite of a careful search, no evidence was seen for ion pair production in lithium. Instead, a very high rate was measured for associative ionization:

$$Li^{**} + Li^{**} \rightarrow Li_2^{+} + e^{-} \qquad (2)$$

Rate constants as high as 5×10^{-7} cm^3 sec^{-1}, close to geometric, were measured for lithium excited to a principal quantum number of 9. This data, together with a new model of associative ionization, was reported previously[1] and has been published.[2]

Negative ions detected in this experiment were deduced to have been formed by attachment to vibrationally excited lithium molecules[3]

$$Li_2(v^*) + e^{-} \rightarrow Li^{-} + Li \qquad (3)$$

The presence of vibrationally excited molecules was a by-product of optically pumping the $Li_2(A-X)$ transition with off-color light close to the 671 nm Li(2s-2p) resonance transition. The $Li_2(A)$ state radiatively decays into vibrationally excited $Li_2(X)$ states, and this route has been used to greatly enhance Li^{-} production in a prior experiment.[4]

One aspect of the experimental data which merited further study was the presence of an extremely rapid rise in Li^- production with optical pump intensity (on the Li(2p-Rydberg) transition) at the point where an optimum existed for Li_2^+ formation.[2] There was not present a similarly large increase in Li^+ (i.e. electron density) and it therefore appeared that some other process could be forming additional $Li_2(v^*)$ molecules in this intensity range, or possibly even that a different mechanism for Li^- production was coming into play. At lower intensities Li^- production had close to a second power dependence on (2p-Rydberg) pump intensity in agreement with the positive ion production, and hence electron production, indicating that attachment was the principal Li^- formation process. At the steepest part of the Li^- production curve a slope of 4 was measured, on a log-log plot against (2p-Rydberg) pump intensity.

The aim of the present work was to investigate the possibility that an additional efficient route to Li^- formation existed in the optically pumped plasma of this experiment. The approach was to continue measurements in the intensity regime that exhibited the steepest slope dependence of Li^- on Li(2p-Rydberg) pump intensity, particularly looking at the time-dependence of Li^- formation, to look for evidence, for example, of an energy transfer to $Li_2(v^*)$:

$$Li^{**} + Li_2(v=0) \rightarrow Li_3^{**} \rightarrow Li_2(v^*) + Li \qquad (4)$$

Another possible mechanism was energy transfer from Li(2p) to $Li_2(v^*)$ via

$$Li(2p) + Li_2(v=o) \rightarrow Li_2(v^*) + Li(2s) \qquad (5)$$

which can occur via the $Li_2(A)$ state because of close energy coincidences of the Li(2s-2p) transition with $Li_2(A-X)$ transitions.

In the event, repeated experimental difficulties were experienced which prevented the acquisition of significant new data. However a theoretical effort was mounted which gave increased insight into the role of electron density increases in possibly causing the rapid negative ion increase. This modeling will be discussed in the following sections.

2.0 KINETIC MODEL OF OPTICALLY PUMPED LITHIUM PLASMA

A kinetic model has been constructed which includes collisional ionization, photoionization, electron collisions and recombination processes. In addition to collisional ionization

$$Li(nl) + Li(nl) \rightarrow Li^{+} + Li + e^{-} \tag{6}$$

there is also at these low beam temperatures a strong component of associative ionization:

$$Li(nl) + Li(nl) \rightarrow Li_2^{+} + e^{-} \tag{7}$$

Rates for processes (6) and (7) are shown in Fig. 1 as broken and continuous curves respectively.

In order to simplify the optical pumping equations it is assumed that at all times electron collisions keep the 2p and nl spin-orbit sub-states mixed among themselves in the ratio of their degeneracies, although this cannot be true at early times. It may then be shown, taking the case of 3d pumping as an example, that

$$\dot{n}_{2p} = \frac{I_{sp}\sigma\,(^2S_{1/2}-^2P_{1/2})\,(5n_{2s}-n_{2p})}{h\nu_{sp}} \tag{8}$$

and

$$\dot{n}_{3d} = \frac{I_{pd}\sigma\,(^2P_{3/2}-^2D_{3/2})\,(2n_{2p}-n_{3d})}{h\nu_{pd}} \tag{9}$$

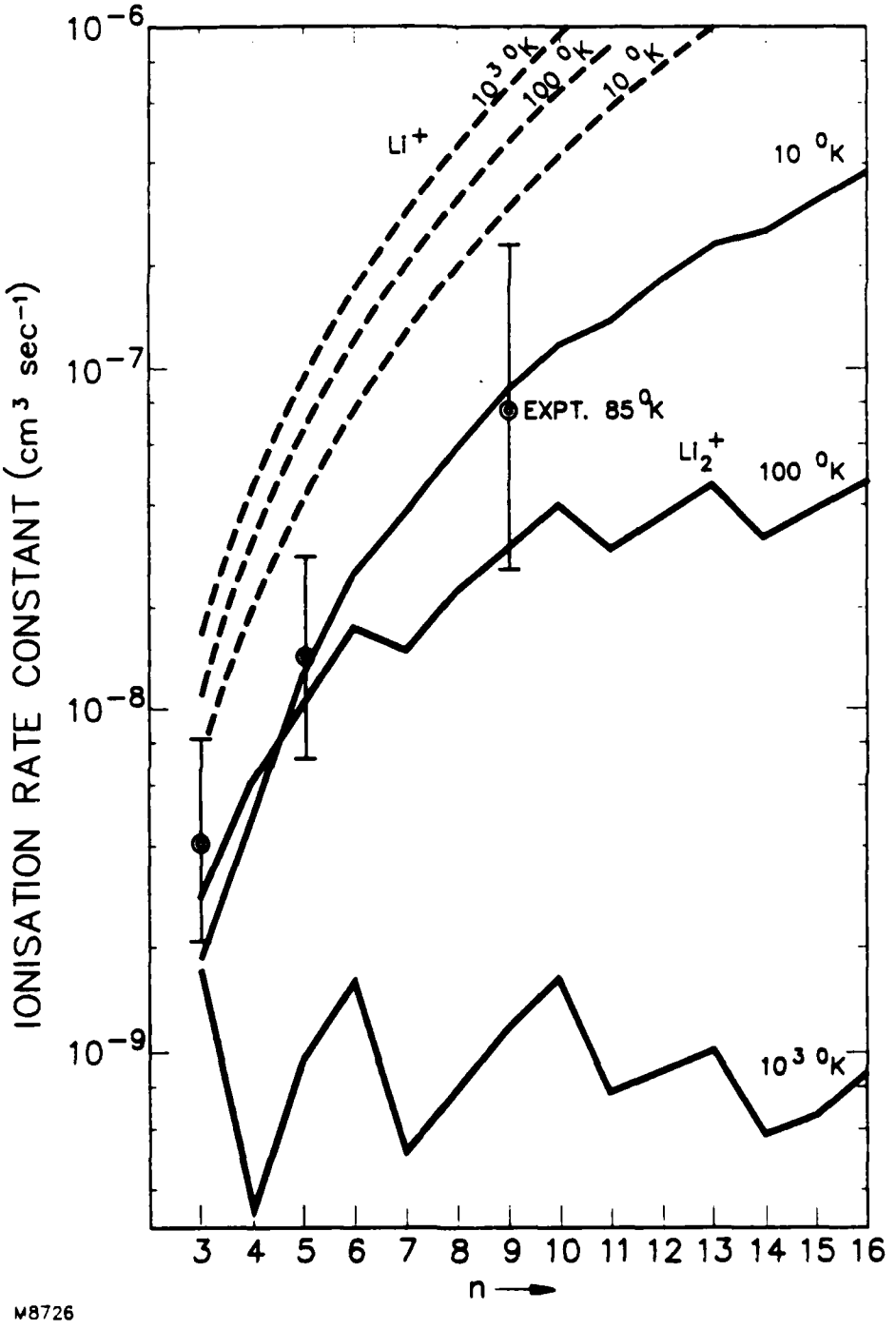

Fig. 1 Illustration of Rates for Collisional Ionization and Associative Ionization as a Function of Principal Quantum Number n. Dashed curves are calculated from Olson (Ref. 9) and full curves from Ref. 2.

where I_{sp} and I_{pd} are the in-band optical pump intensities on the (2s-2p) and (2p-3d) transitions, and ν_{sp}, ν_{pd} are the transition frequencies. Each of the $(^2S_{1/2}-^2P_{1/2})$ and $(^2S_{1/2}-^2P_{3/2})$ subtransitions is pumped by intensity I_{sp} and each of $(^2P_{3/2}-^2D_{3/2})$, $(^2P_{3/2}-^2D_{5/2})$ by I_{pd}. The cross sections are

$$\sigma(^2S_{1/2}-^2P_{1/2}) = 5\times10^{-11}/\sqrt{T}\ \text{cm}^2 \tag{10}$$

$$\sigma(^2P_{3/2}-^2D_{3/2}) = 8\times10^{-11}/\sqrt{T}\ \text{cm}^2 \tag{11}$$

where T is the beam translational temperature in °K.

Electrons in this plasma have a high probability of gaining energy by superelastic collisions, as previously demonstrated in a detailed model for the intense excitation of sodium vapor.[5] Because of the possible importance of hot electrons in one or multiple step ionization of the 3d state the electrons were accounted separately as two groups, those with energy less than 1 eV and greater than 1 eV. Energy relaxation of the hot electrons by e-e collisions becomes important above a cold electron density of ~ 10^9 cm^{-3}, and this process is included.

Radiation trapping is important on the (2p-2s) transition and can also affect the (3d-2p) transition once the 2p population has risen. A (2p-2s) trapping factor of 20 was used, as being representative of experimental conditions in prior work.[2] The (3d-2p) factor was taken as 3, based on 2p densities in a typical simulation. The application of the following results to scale sizes much greater than or less than 1 cm should include a reappraisal of the effect of radiation trapping.

Rates used in the simulation are listed in Table 1. Most of the electron collisional rates are listed as order of magnitude estimates based on the analogy with sodium rates[6] and other estimates of Rydberg collisional rates.[7] The most important contributors to ionization are processes (2) and (7) above. In order to provide a two-step ionization route from Li(3d) to Li^+ an intermediate Li(nl) state is included which is given rates appropriate for the range $5 < n < 10$. Correct treatment of the plasma at densities exceeding 10^{11} cm^{-3} would involve the inclusion of many nl states because a local thermodynamic equilibrium (LTE) is estabished between Li^+ and Li ($n > 5$). It follows that the evolution of these optically pumped plasmas cannot be followed out of the transient regime and into steady state by the present model.

TABLE 1

Index	Process	Rate	Ref.
1	$Li(2s)+h\nu \rightarrow Li(2p)$	$\sigma I_{sp}/h\nu$	-
2	$Li(2p) \rightarrow Li(2s)+h\nu$	$(1/20)*3.72\times10^{7}\,sec^{-1}$	-
3	$Li(2p)+h\nu \rightarrow Li(3d)$	$\sigma I_{pd}/h\nu$	-
4	$Li(3d) \rightarrow Li(2p)+h\nu$	$(1/3)*7.16\times10^{7}\,sec^{-1}$	-
5	$Li(2p)+e_c^- \rightarrow Li(2s)+e_h^-$	$1.5\times10^{-7}\,cm^3\,sec^{-1}$	(e),[6]
6	$Li(3d)+e_c^- \rightarrow Li(2p)+e_h^-$	$2.5\times10^{-7}\,cm^3\,sec^{-1}$	(e)
7	$Li(3d)+e_c^- \rightarrow Li(2s)+e_h^-$	$2\times10^{-8}\,cm^3\,sec^{-1}$	(e)
8	$Li(nl)+e_c^- \rightarrow Li(3d)+e_h^-$	$10^{-6}\,cm^3\,sec^{-1}$	(e),[7]
9	$Li(nl)+e_{c,h}^- \rightarrow Li^+ +2e_c^-$	$10^{-6}\,cm^3\,sec^{-1}$	(e)
10	$Li(3d)+e_h^- \rightarrow Li^+ +2e_c^-$	$2\times10^{-8}\,cm^3\,sec^{-1}$	(e)
11	$e_h^- + e_c^- \rightarrow 2e_c^-$	$(n_{ec}/1056)\,sec^{-1}$	(e)
12	$Li^+ +2e_c^- \rightarrow Li(nl)+Li+e_c^-$	$10^{-26}\,cm^3\,sec^{-1}$	(e)
13	$Li_2^+ + e_c^- \rightarrow Li(nl)+Li(2p)$	$6\times10^{-7}\,cm^3\,sec^{-1}$	e,[8]
14	$Li(3d)+Li(3d) \rightarrow Li^+ +Li(2p)+e_h^-$	$5\times10^{-9}\,cm^3\,sec^{-1}$	[2],[9]
15	$Li(nl)+Li(nl) \rightarrow Li^+ +Li(3d)+e_h^-$	$5\times10^{-7}\,cm^3\,sec^{-1}$	[2],[9]
16	$Li(3d)+Li(3d) \rightarrow Li_2^+ + e_c^-$	$3\times10^{-9}\,cm^3\,sec^{-1}$	[2]
17	$Li(nl)+Li(nl) \rightarrow Li_2^+ + e_c^-$	$1\times10^{-7}\,cm^3\,sec^{-1}$	[2]
18	$Li(nl) \rightarrow Li(3d)+h\nu$	$10^{6}\,sec^{-1}\,(nl=9d)$	(e)
19	$(Li_2^+)^* + e_{c,h}^- \rightarrow Li^+ +Li^+ +2e_c^-$	$10^{-6}\,cm^3\,sec^{-1}$	(e)
20	$Li_2(v^*)+e_{c,h}^- \rightarrow Li^- +Li(2s)$	$2\times10^{-8}\,cm^3\,sec^{-1}$	[3]
21	$Li_2(v^*)+e_c^- \rightarrow Li_2(v=o)+e_c^-$	$10^{-9}\,cm^3\,sec^{-1}$	(e)
22	$Li(3d)+h\nu \rightarrow Li^+ +e_{cold}^-$	$\sigma=6\times10^{-18}\,cm^2$ (610 nm) $\sigma=9\times10^{-18}\,cm^2$ (671 nm)	[10]
23	$Li(3d)+e_h^- \rightarrow Li(nl)+e_c^-$	$10^{-6}\,cm^3\,sec^{-1}$	(e)
24	$Li^+ +Li^- \rightarrow Li(3d)+Li(2s)$	$1.5\times10^{-7}\,cm^3\,sec^{-1}$	(e),[11]

3.0 APPLICATION OF MODEL TO ASSOCIATIVE IONIZATION EXPERIMENT

In this experiment,[1,2] the duration of optical pumping was 3 nsec. In the model runs that follow we employed a 10 nsec duration of optical pumping simply in order to increase the integration stepsize and allow fast turnaround on a desktop computer. This approximation did not materially affect the results, which involve a typical timespan of 1 μsec for excited state-excited state interactions.

In order to review the experimental information we present a typical plot of Li^+, Li_2^+ and Li^- currents versus optical pump intensity on the Li(2p-Rydberg) transition (Fig. 2). A constant saturation optical flux is applied to the Li(2s-2p) resonance transition. We would expect a model to be able to duplicate the slopes (1.8 and 2.2 for Li_2^+ and Li^+ respectively) and the dramatic reduction in Li_2^+ at high pump intensity.

Figure 3 shows the model performance for the data set in Table 1. By comparison with the experiment in Fig. 2 we note that the slopes for Li^+ and Li_2^+ are of the correct order (2) but do not differ from each other. Also the Li_2^+ current begins to decrease at high intensity, but does not decrease dramatically in the way that the experimental data does. A second model run with process (9) of Table 1 increased by an order of magnitude is shown in Fig. 4. This time there is a divergence between the Li^+ and Li_2^+ slopes and a substantial decrease in Li_2^+ at high pump intensity. Apparently the electron avalanche process:

$$Li(nl) + e^- \rightarrow Li^+ + 2e^- \qquad (12)$$

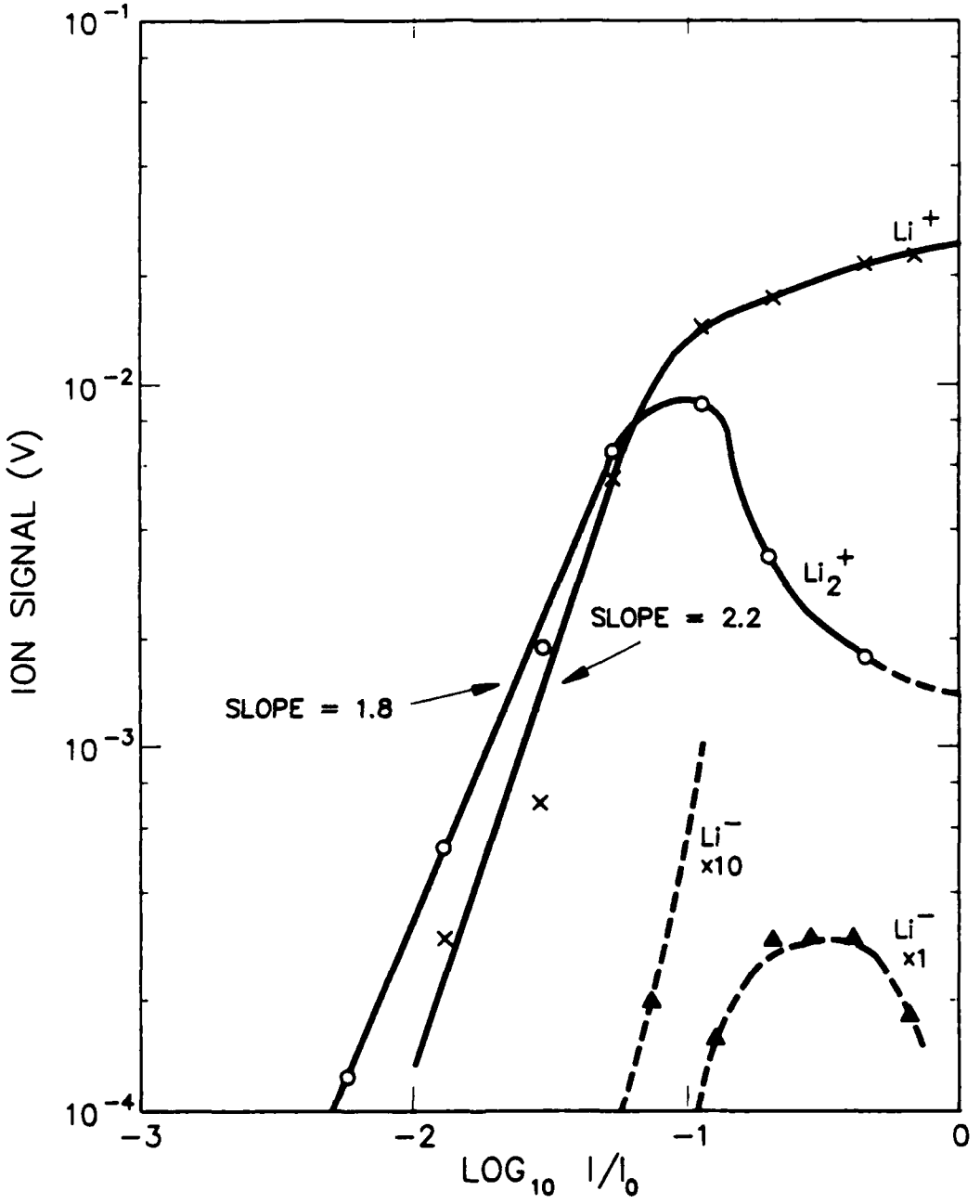

Fig. 2 Measured Li^+, Li_2^+ and Li^- Signals as a Function of Laser Intensity on the 2p-9d Transition at Constant Extraction Time Delay of 2 μsec. Intensity I is normalized to peak intensity I_0.

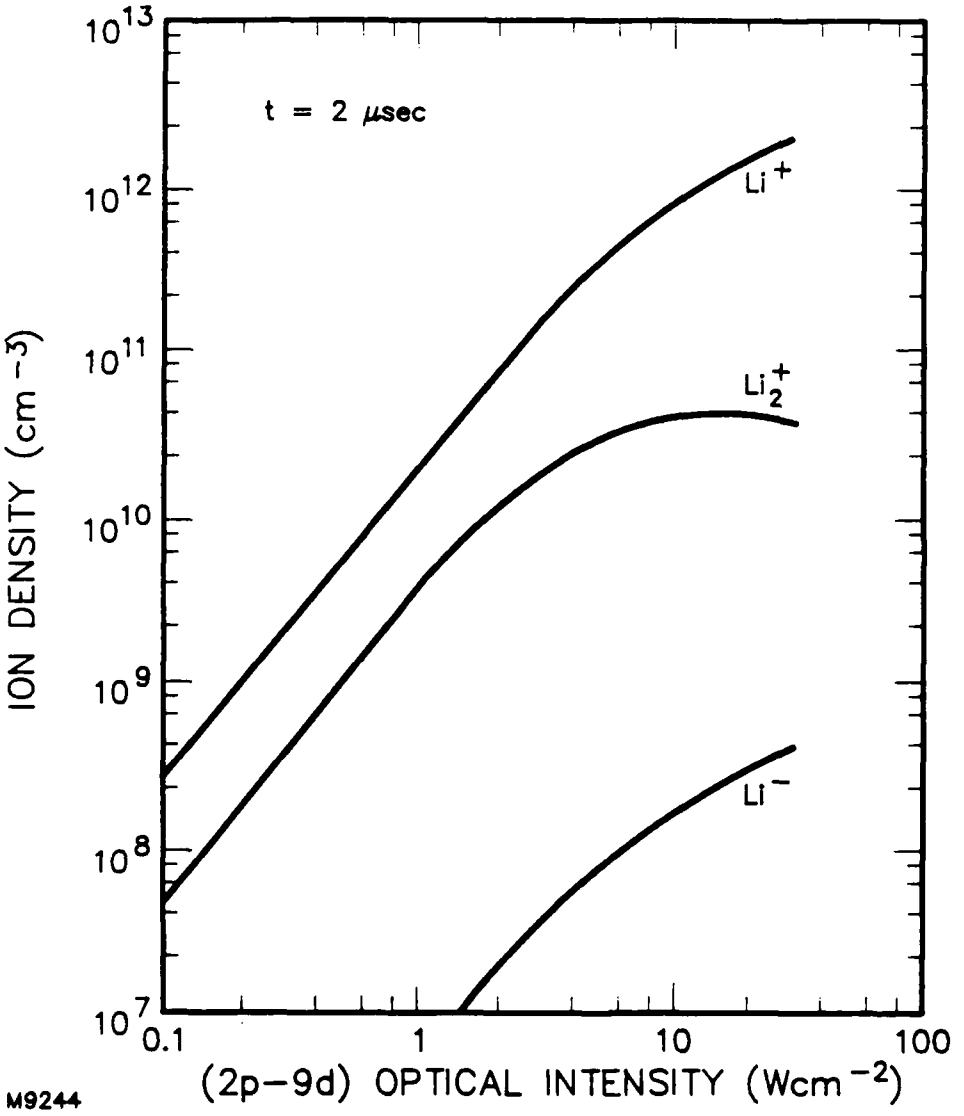

Fig. 3 Model Calculation of Ion Densities 2 μsec After 10 nsec Excitation Pulses of 1 W cm^{-2} on the Li(2s-2p) Transition and Varying Intensity on the (2p-9d) Transition. Rate constants as in Table 1.

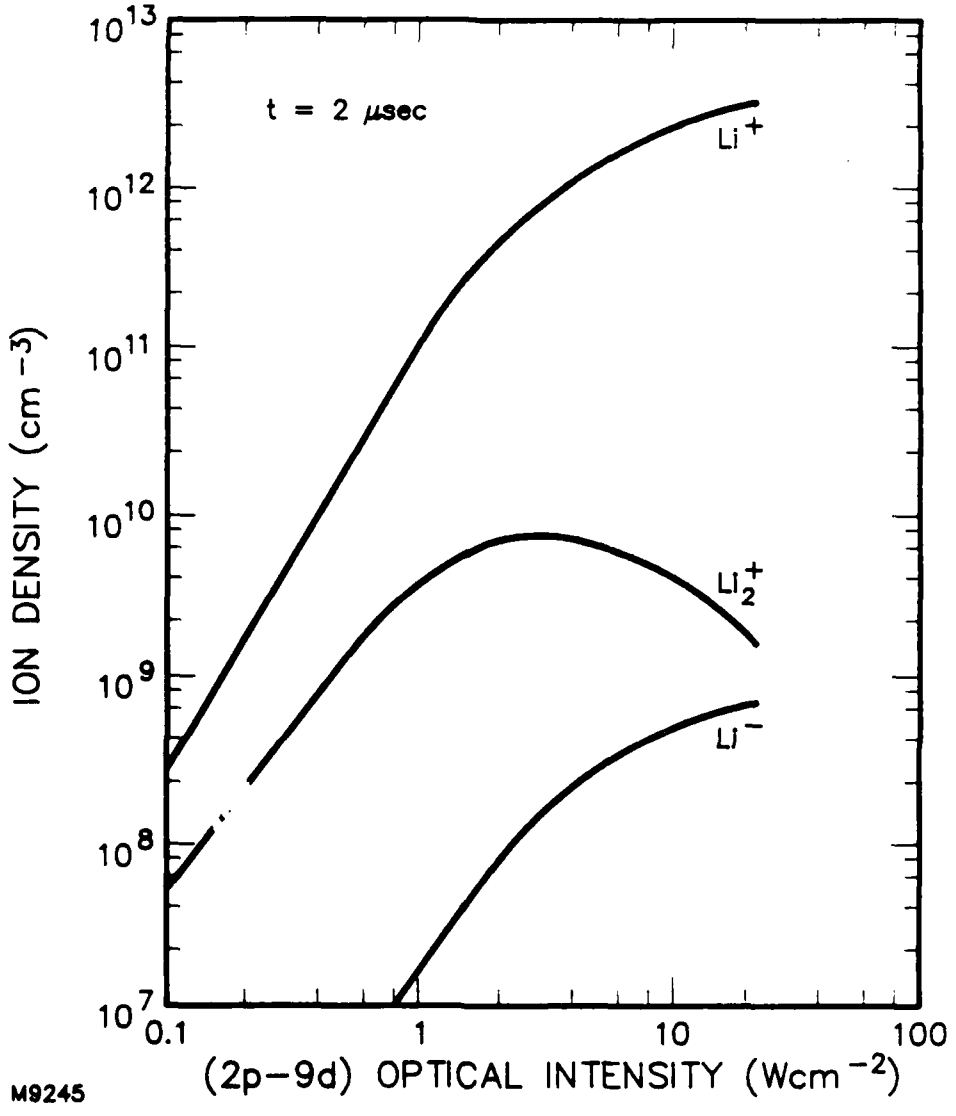

Fig. 4 Model Calculation of Ion Densities 2 μsec After 10 nsec Excitation Pulses of 1 W cm^{-2} on the Li(2s-2p) Transition and Varying Intensity on the (2p-9d) Transition. Rate constants as in Table 1 with the exception that process (index 9) is increased to 10^{-5} cm^3 sec^{-1}. Li^+ slope is 2.4 and Li_2^+ slope is 1.8.

can account for many features of the observations. One major discrepancy remains, however. The model Li^+ signal is one order of magnitude too large relative to Li_2^+. This is a consequence of the relative rates for processes (6) and (7), which are derived from the Olson calculation[9] and experiment,[2] respectively. Rather than accept that the ratio of these rates is incorrect we prefer to believe that the experiment has under-recorded Li^+ relative to Li_2^+, possibly by the mechanism outlined below.

Li^+ is formed by two principal mechanisms, processes (6) and (12) above. At low optical pump intensity process (6) dominates. However, Li^+ ions formed in the latter process carry additional energy, due to their birth on a repulsive potential energy curve of the transient $Li^+...Li(N)$ complex.[2] Because of this energy there is the possibility that many of these Li^+ ions can move outside the acceptance aperture of the time-of-flight mass spectrometer. A sample calculation (Fig. 5) shows the distribution of energy increments that Li^+ ions receive in addition to their original kinetic energy. The net result is that 100°K Li atoms (3/2 kT=0.013 eV) gain approximately the same energy again (on average) through ionization via process (6). This alone accounts for an increase in extracted ion beam divergence of $\sqrt{2}$ times, and a decrease in collection efficiency of 2 times at the 0.5 cm aperture of the channeltron ion detector. An additional loss occurs because the current density of the extracted ion beam is reduced at its source due to lateral expansion of the ions in the 2 μsec before ion extraction. This effect is difficult to quantify, but could be responsible for a further factor of two decrease in collected Li^+ relative to Li_2^+ ions. There is evidence from the time-dependence of the collected Li^+ current that early

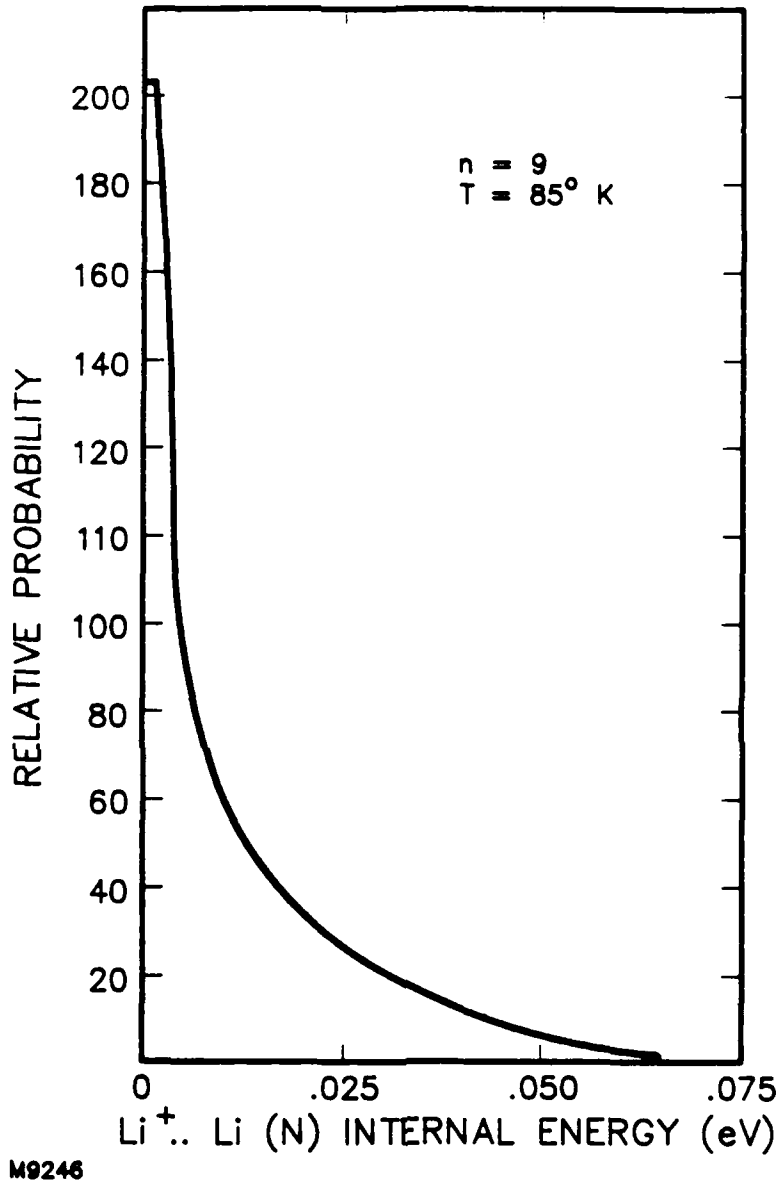

Fig. 5 Distribution of Internal Energy of $Li^+...Li(N)$ Complex During Process of Collisional Ionization.

expansion reduces the Li^+ signal. Figure 6 shows the Li^+ signal for 0.1 μsec and 2 μsec extraction delays. There is approximately a factor of two greater width in the case of immediate extraction, indicating that half the Li^+ ions are not collected after a delay of 2 μsec. The Li^+ pulse is extended on its trailing edge principally because of continued ion production during the 400 nsec duration of the ion extraction pulse.

Overall a factor of 4 inefficiency in Li^+ collection is estimated, and when this factor is applied to the experimental data of Fig. 2 there is reasonable agreement at low optical pump intensities with the model prediction of the Li^+:Li_2^+ ratio. At higher intensities it is possible that Li^+ extraction is inefficient due to ion space charge.

A further variation of model parameters was considered. Runs were made with the data set in Table 1 modified to have a Li(nl) de-excitation rate of 10^{-5} cm^3 sec^{-1} due to electron collisions (process index 8). In this case an electron avalanche does not occur, and Li_2^+ continues to grow with pump intensity in spite of increasing destruction of Rydberg states. The Li^+ and Li_2^+ slopes are equal to 2.0.

In summary, the most convincing explanation of the experimental data of Fig. 2 is the onset of an electron ionization avalanche via process (12). For completeness the time histories of ion production predicted by the model are compared with experiment in Figs. 7 and 8. The Li_2^+ density decreases at late times due to recombination, which is included in the model. Experimentally there are signs of this decrease at higher optical pump intensity.

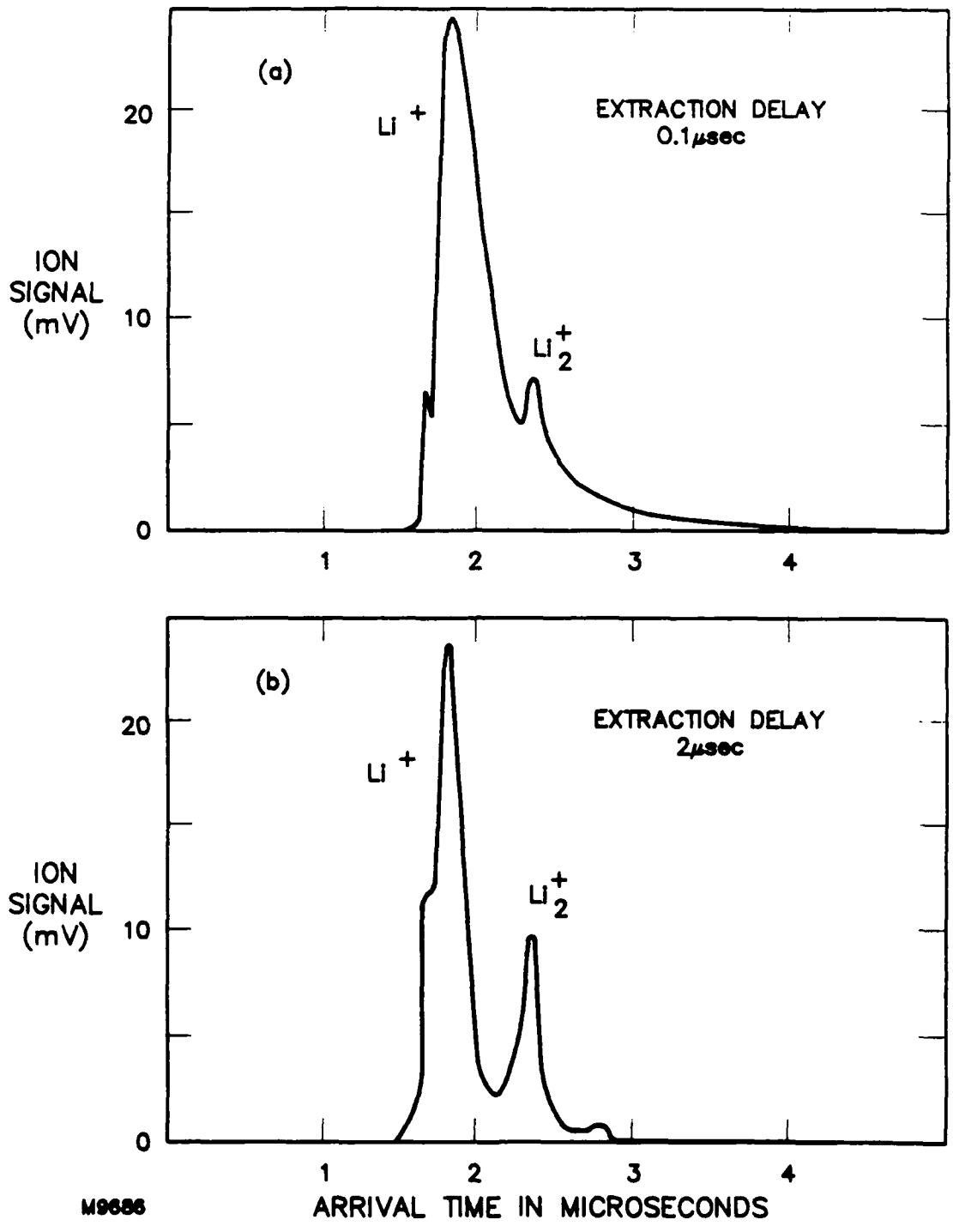

Fig. 6 Time-of-Flight Ion Signals for (a) Extraction Pulse 0.1 μsec After Optical Excitation (b) Extraction Pulse 2 μsec After Optical Excitation, Showing Loss of Li^+ Ions with Later Extraction

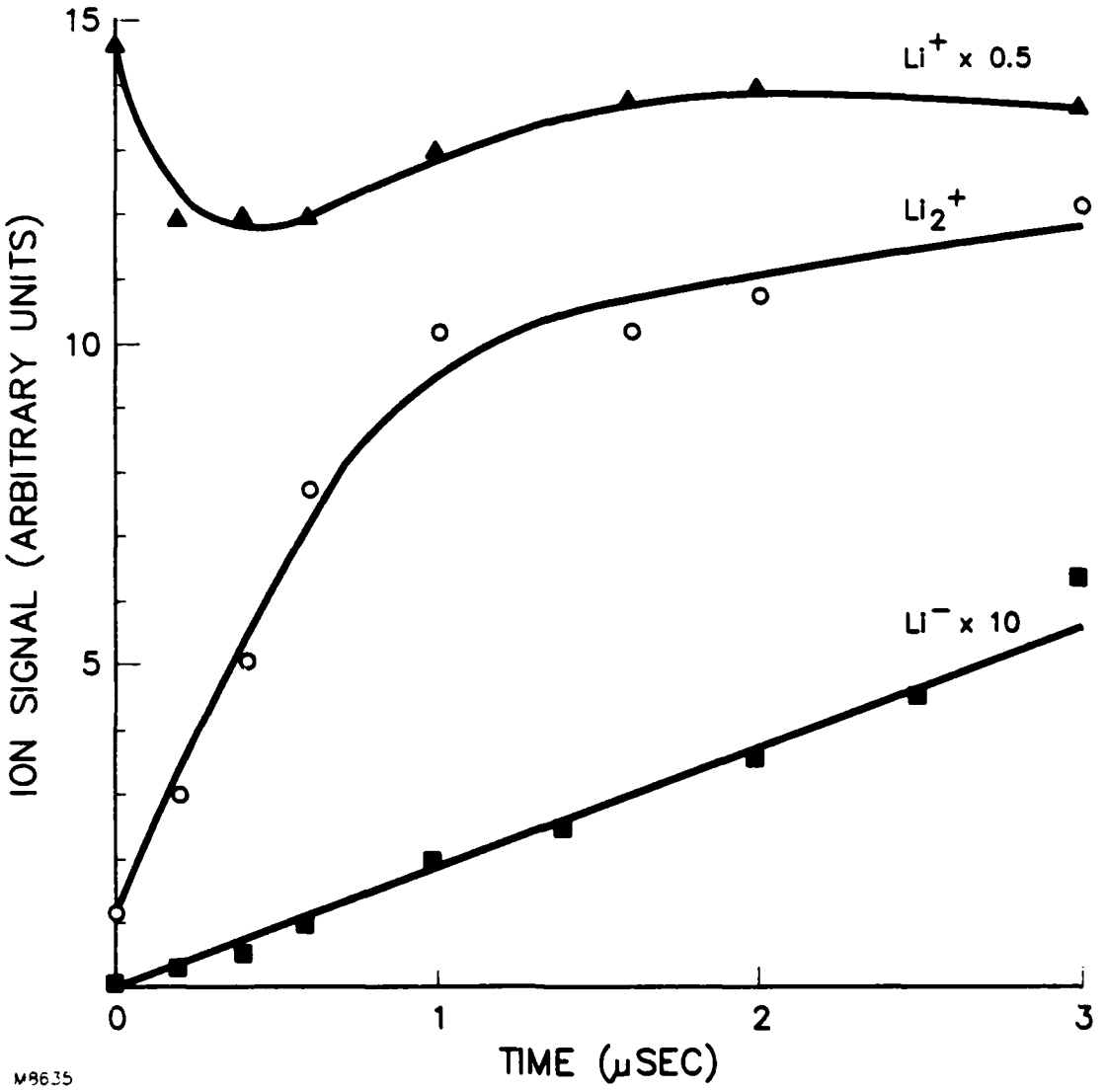

Fig. 7 Measured Dependence of Li^+, Li_2^+ and Li^- Signals with Delay Before Ion Extraction

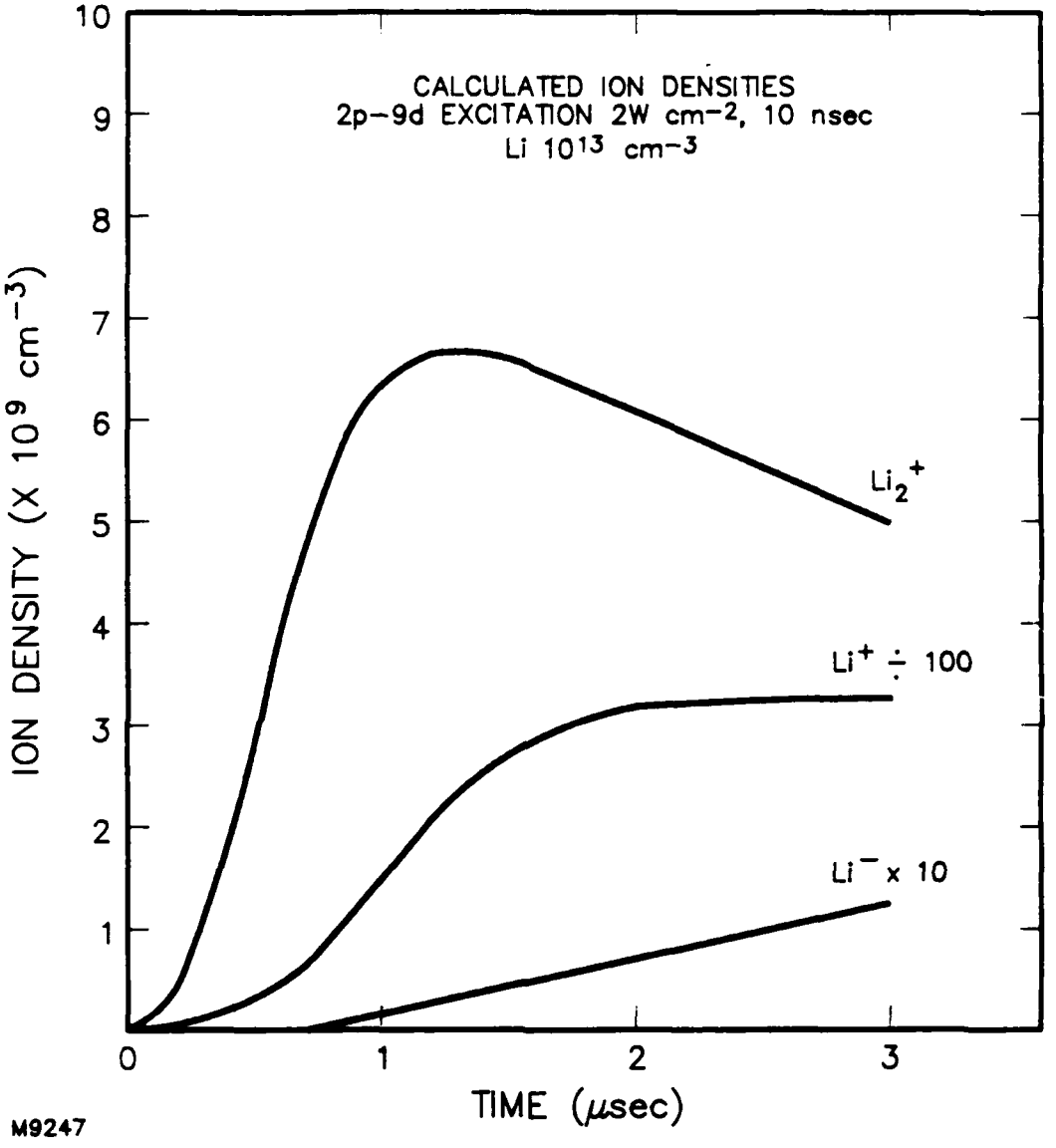

Fig. 8 Model Calculation of Ion Densities as a Function of Delay After Excitation on the Li (2s-2p) and (2p-9d) Transitions, with 1 W cm^{-2} and 2 W cm^{-2} Respectively for a Duration of 10 nsec

4.0 APPLICATION OF MODEL TO CONTINUOUS OPTICAL PLASMA PRODUCTION

In application of the model to the optical pumping of a supersonic lithium beam[12] the interaction time is limited by the transit velocity of the beam, which is ~ 3 x 10^5 cm sec^{-1} (Ref. 3). For the purposes of discussion an optical pump duration of 1 μsec is chosen. Two-step excitation to the Li(3d) state is considered. The electron density at 1 μsec is shown as a function of the two pump intensities in Fig. 9. After 1 μsec has elapsed the fractional ionization can reach several percent. Approximately ten times greater intensity is required on the (2p-3d) transition than on the (2s-2p) transition in order to reach saturating ionization. The time evolution of the electron density is shown in Fig. 10. Although initially the hot electrons dominate, energy relaxation ensures that more than 97 percent of electrons are cold at 1 μsec.

If it is postulated that all the Li_2 molecules in the beam (4 percent, or more, of the total number density) have been optically pumped[4] to vibrationally excited states $Li_2(v^*)$ which have a high rate of attachment, then high densities of Li^- can form. In Fig. 11 the Li^- density is shown as a function of Li beam density at time 2 μsec after the end of a 1 μsec period of optical pumping. The increasing beam density is acompanied by increasing plasma and Li^- density, at the fixed optical excitation intensities of 0.1 W cm^{-2} and 1 W cm^{-2} on the 2s-2p and 2p-3d transitions respectively. A limit to Li^- density is reached due to the mutual neutralization process

$$Li^+ + Li^- \rightarrow 2Li \qquad (13)$$

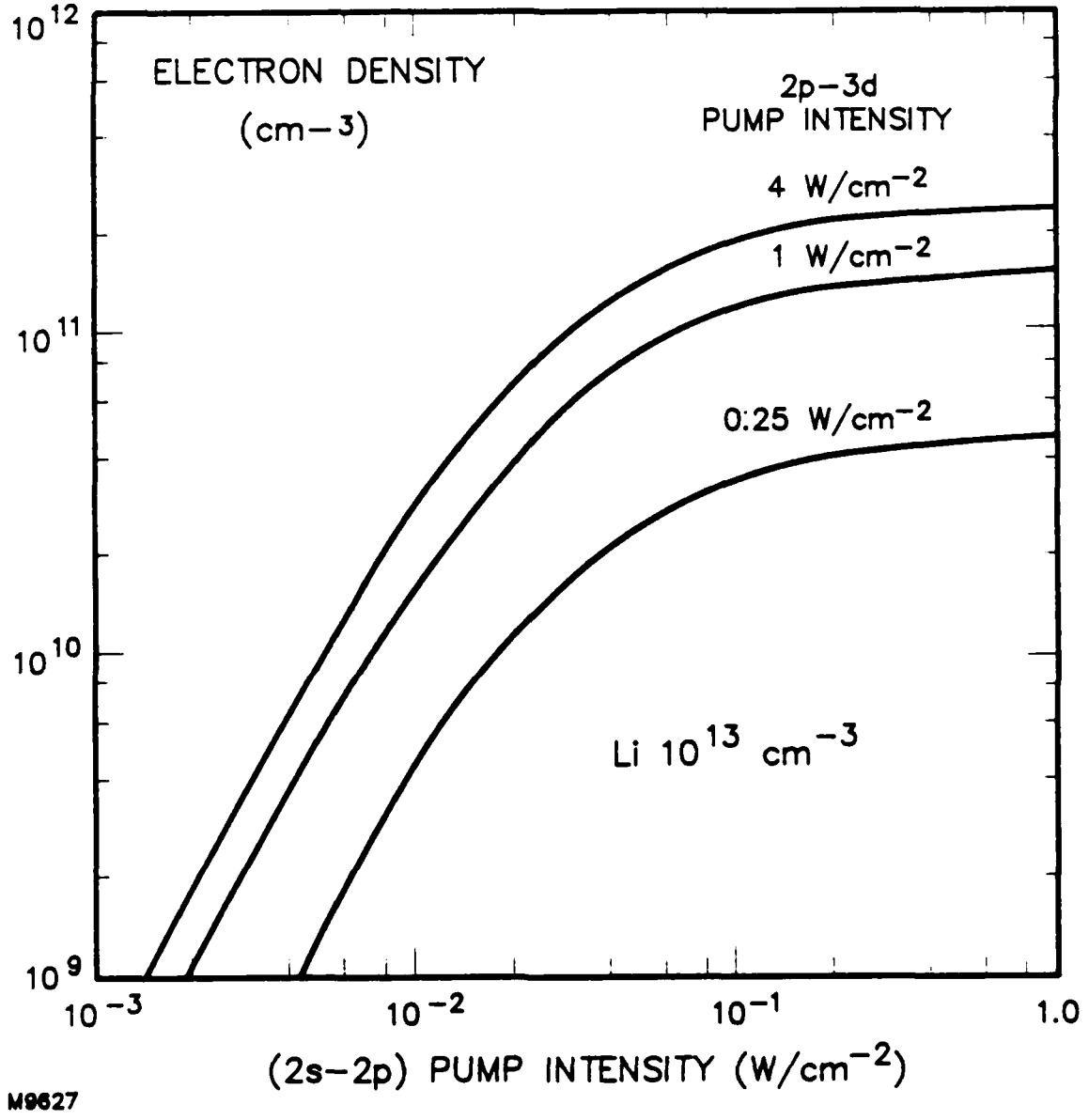

Fig. 9 Electron Density After 1 μsec of Simultaneous Optical Pumping on the Li(2s-2p) and Li(2p-3d) Transitions, as a Function of the Intensity of Each Pump

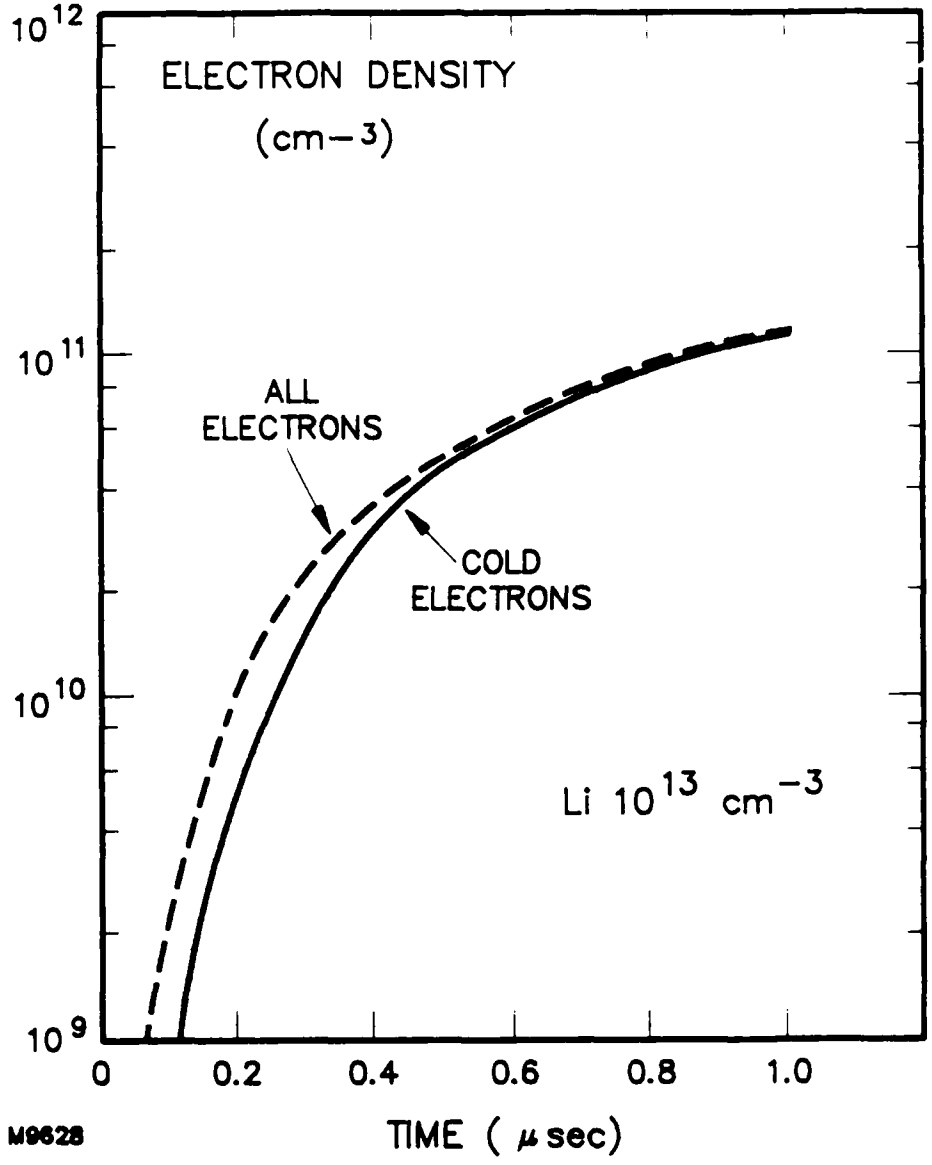

Fig. 10 Evolution of Hot and Cold Electron Populations in 1 μsec After Switch-On of 0.1 W cm^{-2} on (2s-2p) and 1.0 W cm^{-2} on (2p-3d)

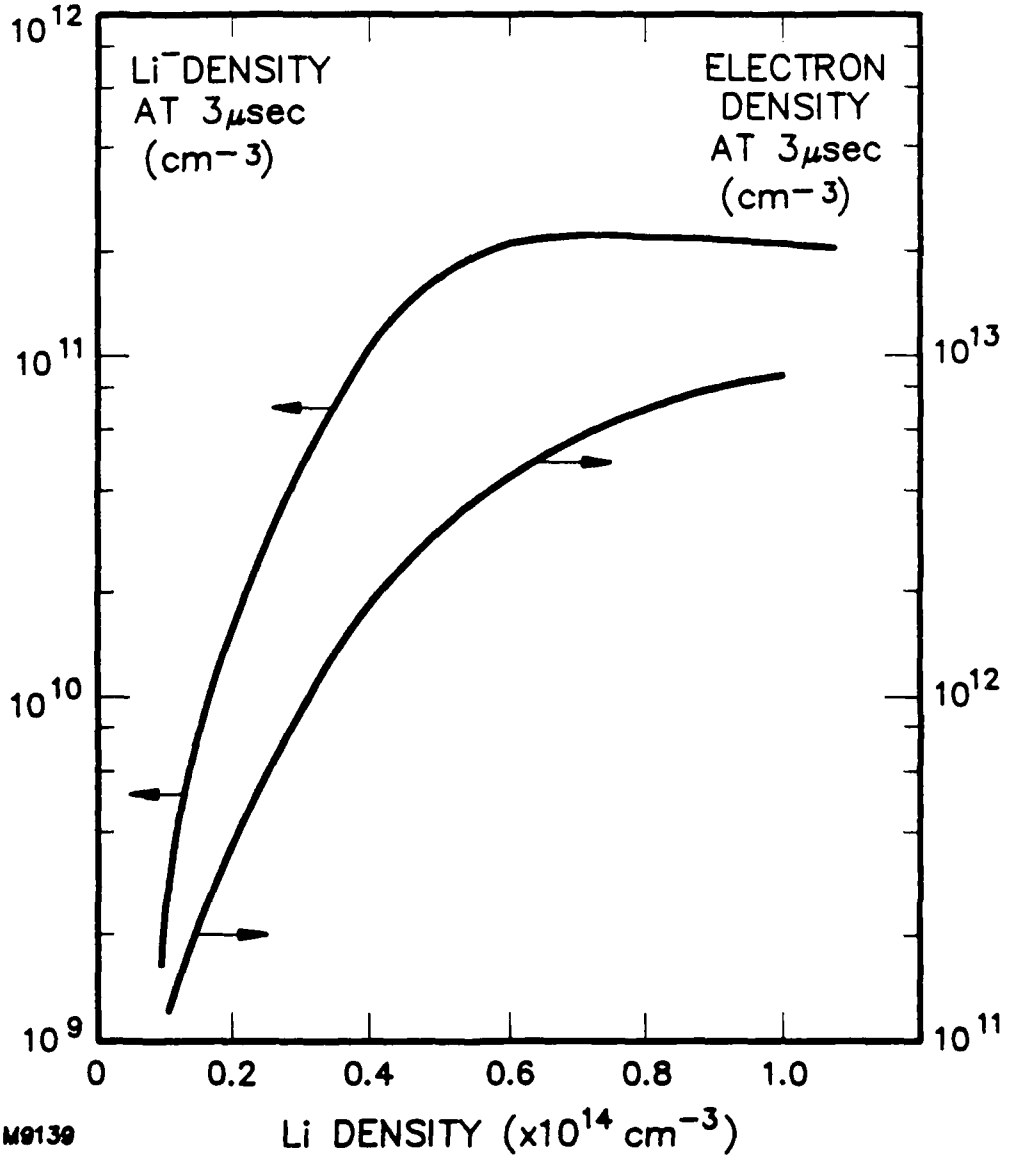

Fig. 11 Li^- and Electron Density 2 μsec After the End of 1 μsec Pumping with 0.1 W cm^{-2} on (2s-2p) and 1.0 W cm^{-2} on (2p-3d). Li density varied from 1 x 10^{13} cm^{-3} to 1 x 10^{14} cm^{-3} with 4% vibrationally excited Li_2

Because of the high beam translational velocity (3×10^5 cm sec^{-1}) the peak Li^- density of 2.2×10^{11} cm^{-3} corresponds to a Li^- current density of 10 mA cm^{-2}.

It is of interest to minimize the ratio of electrons to Li^- ions in order to improve the quality of the extracted ion beam. This may be achieved by maintaining high Li and hence $Li_2(v^*)$ density while reducing the 2p-3d pump intensity. Figure 12 illustrates that the reduced electron density leads to a delayed maximum in Li^- density, the delay exceeding 20 μsec in some cases. At a beam translational velocity of 3×10^5 cm sec^{-1} the Li^- density can peak several cm downstream of the excitation region. The actual peak of Li^- density occurs when destruction by mutual neutralization equals formation by dissociative attachment. The ratio of electrons to negative ions can be reduced to about unity without much reduction in Li^- current density.

In summary, a plasma density of between 10^{11} and 10^{12} cm^{-3} can be continuously generated in a lithium beam of 10^{13}-10^{14} Li atoms cm^{-3} by the use of less than 1 W cm^{-2} on each of the (2s-2p) and (2p-3d) transitions. The dominant ionization mechanisms are collisional and associative ionization of Li(3d) atoms. Negative ions can form at densities up to 2×10^{11} cm^{-3}, limited only by mutual neutralization with positive ions and by the supply of vibrationally excited Li_2 molecules. The electron density can be reduced to below the negative ion density without much reduction in Li^- current density.

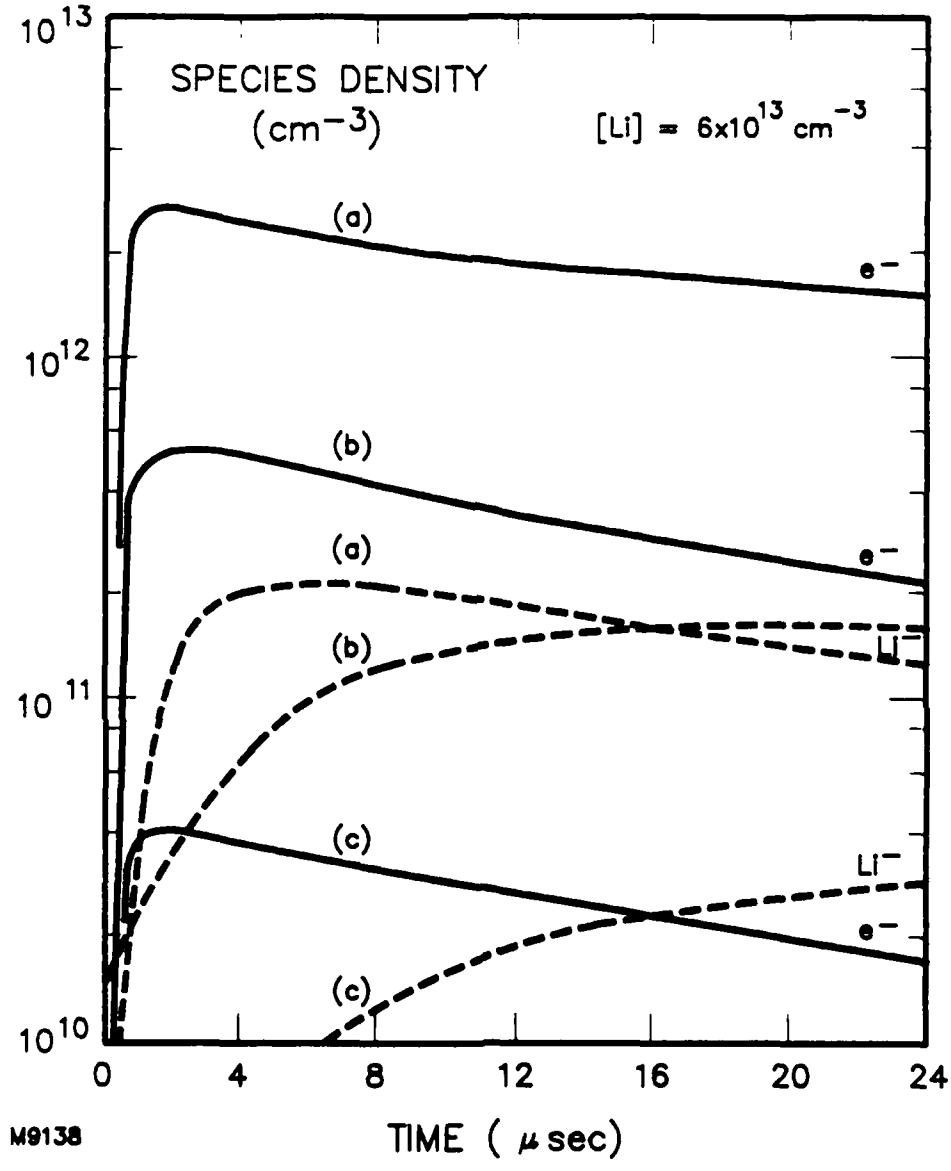

Fig. 12 Time Evolution of Li^- and Electron Densities for Different 1 μsec Optical Excitation Cases Each with 0.1 W cm^{-2} Incident on the (2s-2p) Transition: (a) 0.5 W cm^{-2} on (2p-3d); (b) 0.125 W cm^{-2} on (2p-3d); (c) 0.03 W cm^{-2} on (2p-3d). Li density 6 x 10^{13} cm^{-3} with 4% vibrationally excited Li_2.

5.0 CONCLUSIONS

Several features of the experiments with optically pumped Rydberg atoms are described well by the kinetic model presented above. In particular it appears that an electron avalanche can occur at sufficiently high Rydberg density ($> 10^{11}$ cm^{-3} for n=9). The model predicts more Li^+ than we observe, but it is possible that Li^+ is under-recorded relative to Li_2^+ because of its kinetic energy of formation in the collisional ionization process.

The application of the model to a continuously pumped lithium supersonic beam showed that modest laser powers (< 1 W) were sufficient to maintain a high fractional ionization. On the hypothesis that continuous optical pumping also created vibrationally excited Li_2 molecules a relatively high Li^- current density (10 mA cm^{-2}) is projected, produced at up to and exceeding unity ratio of negative ions to electrons.

6.0 REFERENCES

1. M. W. McGeoch, R. E. Schlier and G. K. Chawla, Report 'Optical Production of Negative Ions,' contract F49620-87-C-0080, period 7-15-87 to 4-14-88 (1988).

2. M. W. McGeoch, R. E. Schlier and G. K. Chawla, "Associative ionization with cold Rydberg lithium atoms," Phys. Rev. Lett. 61, 2088 (1988).

3. M. W. McGeoch and R. E. Schlier, "Dissociative attachment in optically pumped lithium molecules," Phys. Rev. A 33, 1708 (1986).

4. M. W. McGeoch and R. E. Schlier, "Generation of lithium negative ions in a volume source with optical pumping," J. Appl. Phys. 61, 4955 (1987).

5. W. L. Morgan, "Non-Maxwellian electrons in a laser produced sodium plasma," Appl. Phys. Lett. 42, 790 (1983).

6. R. Shuker, A. Gallagher and A. V. Phelps, "Models of high-power discharges for metal-Xe excimer lasers," J. Appl. Phys. 51, 1306 (1980).

7. F. Devos, J. Boulmer and J.-F. Delpech, "Transitions between Rydberg levels of helium induced by electron and neutral collisions," Le Journal de Physique, 40, 215 (1979).

8. By analogy with H_2^+ data of D. Auerbach, R. Cacak, R. Caudino, T. D. Gaily, C. J. Keyser, J. Wm. McGowan, J. B. A. Mitchell and S. F. J. Wilk, "Merged electron-ion beam experiments I. Method and measurements of (e-H_2^+) and e-H_3^+) dissociative-recombination cross sections," J. Phys. B: Atom. Molec. Phys., 10, 3797 (1977).

9. R. E. Olson, "Ionization cross sections for Rydberg atom-Rydberg atom collisions," Phys. Rev. Lett. 43, 126 (1979).

10. A. Burgess and M. J. Seaton, "A general formula for the calculation of atomic photo-ionization cross sections," Mon. Not. Roy. Astron. Soc. 120, 121 (1960).

11. B. M. Smirnov, 'Negative Ions' (McGraw Hill, New York, 1982), Chap. 5.

12. M. W. McGeoch, "Processes in a Lithium Negative Ion Source," presented at SPIE symposium, on Innovative Science and Technology, Los Angeles, January 1989.